ЖЭТФ, 2024, том 166, вып. 4 (10), стр. 566–570

DETECTION OF METRONIDAZOLE AND FAMPRIDINE BY NMR AT ZERO AND ULTRALOW MAGNETIC FIELD

D. B. Burueva [a*], ***J. Eills*** [b,c,d], ***R. Picazo-Frutos*** [b,c,d], ***K. V. Kovtunov*** [a], ***D. Budker*** [b,c,d,e], ***I. V. Koptyug*** [a**]

[a] *International Tomography Center*
Siberian Branch of Russian Academy of Sciences
630090, Novosibirsk, Russia

[b] *Helmholtz-Institut Mainz*
55099, Mainz, Germany

[c] *GSI Helmholtzzentrum für Schwerionenforschung GmbH*
64291, Darmstadt, Germany

[d] *Institute of Physics, Johannes Gutenberg-Universität*
55128, Mainz, Germany

[e] *Department of Physics, University of California*
CA 94720-7300, Berkeley, USA

Received May 15, 2024
revised version May 15, 2024
Accepted for publication June 18, 2024

In this work the biocompatible molecules — metronidazole and fampridine — were successfully hyperpolarized using parahydrogen via the signal amplification by reversible exchange approach. The nuclear magnetic resonance (NMR) signals from both molecules were detected at zero- to ultralow magnetic field (ZULF) using commercially available rubidium vapor magnetometer from QuSpin.

This paper is published as part of the Proceedings of the Conference «Physics of Ultracold Atoms» (PhUHA-2023), Novosibirsk, December 2023

DOI: 10.31857/S0044451024100134

1. INTRODUCTION

Nuclear magnetic resonance spectroscopy is a powerful analytical tool to ascertain structure, dynamics and chemical environment of molecules. NMR is extensively used in chemistry, physics and related fields in both industrial and academic settings. Magnetic resonance imaging (MRI), a modality of NMR with spatial resolution, is also routinely used for diagnostic visualization in medicine.

In conventional NMR, the signal is detected using inductive coupling, whereby the sample of interest is placed in a static magnetic field (B_0) and the Larmor precession of nuclear spins induces an electromotive force (EMF) in a detection coil, which is part of a resonant circuit. In general, NMR is a relatively low-sensitivity spectroscopic technique due to an inherently low degree of nuclear spin polarization (P) with respect to the applied magnetic field. For the most sensitive stable nucleus, proton ^{1}H, the spin polarization in thermal equilibrium is on the order of $10^{-4} - 10^{-5}$ in the magnets of modern NMR instruments at room temperature; for other nuclei with smaller gyromagnetic ratio (γ) the polarization is even lower. Both the EMF and the thermal nuclear spin polarization are proportional to the magnetic field; thus, standard NMR typically operates at high magnetic fields (up to 28 T) to benefit from higher sensitivity and higher chemical shift dispersion. This makes NMR beyond a specialized laboratory environment an uncommon practice.

* E-mail: burueva@tomo.nsc.ru
** E-mail: koptyug@tomo.nsc.ru

At the same time, in addition to the continuing trend in induction-detected NMR toward higher sensitivity and instrumentation complexity, relatively low-field (down to the Earth's field) implementations of NMR are of significant interest beyond laboratory settings [1], in industry [2], petrophysics and logging [3].

Meanwhile, non-inductive schemes for NMR detection are being developed that do not require high magnetic fields. These techniques operate at low and ultralow field enabling the direct detection of the oscillations of sample magnetization. Several approaches have been implemented for NMR detection using superconducting quantum interference devices (SQUIDs) [4], single nitrogen vacancy (NV) centers in diamond [5], and atomic magnetometers [6]. Optically-pumped magnetometers are highly sensitive NMR sensors that can operate at near-zero field within magnetic shielding. The intramolecular spin-spin interactions are predominant in such magnetic fields, while the Zeeman interaction can be considered as a perturbation. Complementary to classical high-field NMR, zero- to ultralow-field (ZULF) NMR offers several advantages. In particular, the setup can be relatively inexpensive and portable as no superconducting magnet and no cryogenics are required. Such low-frequency NMR detection approaches attract significant attention as a platform for developing compact NMR devices [7]. Furthermore, ZULF NMR is free from susceptibility effects and chemical fingerprinting is available even for heterogeneous or multiphasic samples (e.g., with gas-liquid, gas-liquid-solid interfaces) inside electrically conductive materials such as metal containers [8]. In ZULF NMR the sensitivity issues are often solved via field-cycling techniques, e.g., preliminary magnetization of the sample in a magnetic field of 1-2 T (typically produced with permanent magnets) with the subsequent transfer of the sample to ZULF for detection. However, nuclear spin hyperpolarization [9] methods can be alternatively used for this purpose, and both dissolution dynamic nuclear polarization [10] and parahydrogen-based hyperpolarization techniques [11] have been already demonstrated in the context of ZULF NMR.

Parahydrogen-induced polarization (PHIP) [12] technique utilizes parahydrogen (p-H_2; the nuclear spin isomer of molecular hydrogen with the total spin of 0) as a versatile source of hyperpolarization. The correlated state of the nuclear spins of p-H_2 can be inherited by p-H_2-derived protons in a product molecule produced via catalytic hydrogenation of a suitable precursor. Alternatively, the singlet state of p-H_2 can be used to hyperpolarize a molecule of interest by reversible exchange of p-H_2 and the target molecule on a catalyst (usually, a metal complex of Ir) by means of spin-polarization transfer from p-H_2-derived hydrides to the target nuclei. This phenomenon is named signal amplification by reversible exchange (SABRE) [13]. The SABRE method opened the door to a new class of molecules to be hyperpolarized; the main requirement is the ability of a polarizable molecule to bind with a polarization-transfer catalyst. This requirement is typically fulfilled for heterocycles containing an electron-donating heteroatom, such as nitrogen [14]. Importantly, N-heterocyclic structures are a common building block for drugs and biomolecules. A number of biocompatible molecules including nicotinamide [15, 16], pyrazinamide [17], pyridazine derivatives [18], nitroimidazoles [19, 20] have been successfully hyperpolarized. SABRE arouses much interest as a promising hyperpolarization method for ultrafast and inexpensive production of hyperpolarized contrast agents for biomedical magnetic resonance imaging [21, 22]. In turn, ZULF NMR offers a unique modality for *in situ* NMR detection and monitoring SABRE response during the process optimization since such setup is portable and free from hyperpolarization losses associated with sample transfer. From the first ZULF NMR detection of SABRE-hyperpolarized signals [23] this field is expanding and far reaching; using ZULF NMR it became possible to elucidate the SABRE magnetic field profiles [24], monitor the catalyst activation [25], and optimize further relay of SABRE hyperpolarization to other molecules [26]. Thus, the combination of SABRE and ZULF NMR has shown itself to be a practically convenient and productive experimental modality.

In this work, we demonstrate the feasibility of detection of metronidazole and fampridine (another nonproprietary name is dalfampridine; the chemical name is 4-aminopyridine) by NMR at zero- and ultralow magnetic fields. ^{15}N-labeled substrates were used in order to increase the sensitivity. [$^{15}N_3$]Metronidazole and [^{15}N]fampridine were obtained using previously described synthetic procedures (see the Experimental Section for details). Their chemical structures are presented in Fig. 1 *a*. Both molecules were hyperpolarized using the SABRE procedure. During the SABRE process the substrate of interest remains chemically unaltered and its hyperpolarization builds up due to the following steps: 1) activation of Ir complex under H_2 atmosphere and an excess of the substrate. 2) The substrate and the p-H_2-derived hydrides come into temporary contact on the iridium metal center. 3) Polarization transfer occurs in the formed active SABRE complex through the J-coupling network. 4) The re-

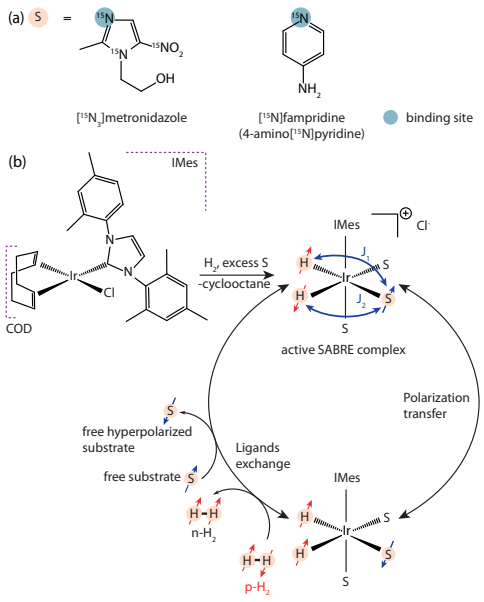

Fig. 1. *a* — The chemical structures of the studied molecules. *b* — The scheme illustrating SABRE approach. The SABRE precatalyst is [Ir(IMes)(COD)Cl], where COD is 1,5-cyclooctadiene and IMes is 1,3-bis(2,4,6-trimethylphenyl)imidazol-2-ylidene. The SABRE precatalyst converts into the active complex in the presence of molecular hydrogen and an excess of substrate

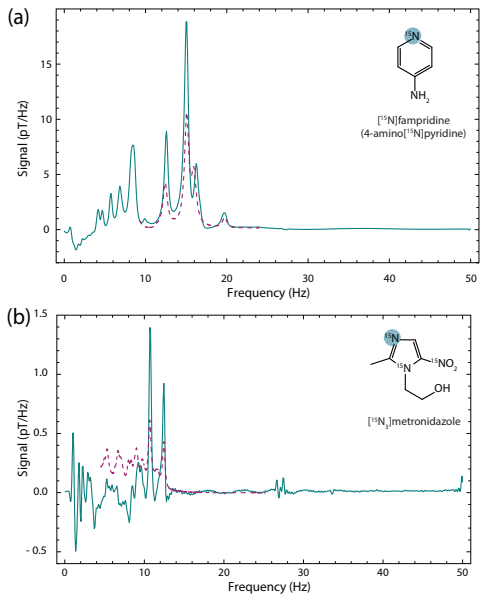

Fig. 2. The low-frequency NMR signals detected at ultralow field (<40 nT) from (*a*) [^{15}N]fampridine and (*b*) [^{15}N$_3$]metronidazole hyperpolarized via signal amplification by reversible exchange with parahydrogen. Each spectrum is the result of 200 averages. Insets show the chemical structures of corresponding substrates. The signal at 27 Hz arises due to electronic noise from the QuSpin zero-field atomic magnetometer. The dotted lines show corresponding simulated spectra

versible exchange of substrate and p-H_2 with their free counterparts in the solution leads to hyperpolarization buildup on the free substrate. The SABRE process is schematically depicted in Fig. 1 *b*.

Both molecules are FDA-approved drugs. Fampridine is a specific blocker of potassium ion channels and a clinically approved drug for the symptomatic treatment of patients with multiple sclerosis [27]. Metronidazole is an important and widely used antiprotozoal drug [28]. Both molecules can be potentially used as hyperpolarized MRI tracers for detection of altered metabolic conditions: metronidazole can be used as an MRI sensor of hypoxia conditions based on its metabolic transformation in O_2-starved tissues [19, 29, 30]; fampridine, in turn, can be potentially used for the MRI detection of demyelinated lesions [31]. The fast production of long-lived hyperpolarized metronidazole and fampridine in large quantities is of interest for the development of new test assays in biological research and MRI monitoring of metabolism *in vivo*, and ZULF NMR is a promising platform for inline monitoring of the SABRE process. As mentioned above, under ZULF conditions, the Zeeman interactions (which dominate in the classical NMR experiment) can be considered as a perturbation with respect to the J-coupling interactions between the nuclei of the studied molecules and dipole-dipole interactions. In this case, the so-called J-spectrum is obtained, which can be complex and sensitive to changes in the geometry, conformation and electronic state of the molecule under study.

In this work, the J-spectra from SABRE-hyperpolarized metronidazole and fampridine were acquired using commercially available QuSpin zero-field atomic magnetometer [32], the principle of which is based on optical pumping and probing atomic rubidium [33]. The experimentally detected ZULF NMR spectra of [^{15}N$_3$]metronidazole and [^{15}N]fampridine are shown in Fig. 2. Both the NMR sample tube and the magnetometer were placed inside the four-layer magnetic shield and the sensor was positioned near the side of the NMR tube [34].

The obtained J-spectra are directly related to the J-coupling interactions in the studied molecules. For [^{15}N]fampridine (or 4-amino[^{15}N]pyridine), the strongest J-coupling is $^2J_{\mathrm{NH}}$ between ^{15}N in the pyridine ring and the two ortho-protons, and the ^{14}N nucleus (in the amino group) can be disregarded due to self-decoupling via fast quadrupolar relaxation.

Thus, the main peak for [^{15}N]fampridine appears at $3/2 \times {}^2J_{\mathrm{NH}}$ [35], which corresponds to 15 Hz. The long-range couplings to other protons result in the appearance of additional sidebands signals. The signal-to-noise ratio of the peak at 15 Hz after 200 averages is 2000. For [$^{15}N_3$]metronidazole the J-spectrum is more complex due to a lower molecular symmetry and a larger spin system (11-spin system). The ${}^2J_{\mathrm{NH}}$ between the ^{15}N nucleus and one ^{1}H in the imidazole ring is 9 Hz resulting in the signal appearing at $1 \times {}^2J_{\mathrm{NH}} = 9$ Hz. However, the other J-couplings in the molecule produce a number of additional sidebands and a shift of the largest peak to 10.5 Hz. It should be mentioned that all spectra were acquired during continuous p-H_2 bubbling through the solution which did not deleteriously affect the spectral resolution. The linewidths in the spectra are Fourier-transform limited by a 3 s signal-acquisition time.

In conclusion, ZULF NMR offers a unique modality for *in situ* NMR detection and monitoring of SABRE response during the process optimization. In this work, two ^{15}N-labeled biocompatible molecules, namely [$^{15}N_3$]metronidazole and [^{15}N]fampridine (also known as 4-amino[^{15}N]pyridine), were hyperpolarized using parahydrogen via signal amplification by reversible exchange. We demonstrate the possibility to acquire ZULF NMR spectra from hyperpolarized metronidazole and fampridine using the setup equipped with a commercially available QuSpin zero-field magnetometer. The J-spectra were acquired while p-H_2 was constantly bubbled through the solution, highlighting the robustness of ZULF-NMR detection.

2. EXPERIMENTAL

^{15}N-labeled metronidazole and fampridine were obtained using previously described synthetic procedures: the synthesis of [$^{15}N_3$]metronidazole is described in Ref. [19]; the synthesis of [^{15}N]fampridine (or 4-amino[^{15}N]pyridine) is described in Ref. [36]. Methanol was used as received. The iridium complex [Ir(IMes)(COD)Cl] (where COD is 1,5-cyclooctadiene and IMes is 1,3-bis(2,4,6-trimethylphenyl)imidazol-2-ylidene) was obtained using the preparation procedure described elsewhere [37]. The initial solution was 5 mM [Ir(IMes)(COD)Cl] and 25 mM substrate ([^{15}N]fampridine or [$^{15}N_3$]metronidazole) in 300 μL methanol. The activation of the SABRE complex took 30 min.

Parahydrogen at >96 % enrichment was generated by passing hydrogen gas over hydrated iron(III) oxide catalyst (30–50 mesh, Sigma-Aldrich) in a closed-cycle cryostat operating at 30 K (Advanced Research Systems). For all NMR experiments, parahydrogen-enriched gas was continuously bubbled through the sample at 5 bar and the signal was acquired for 3 s after applying a magnetic field pulse centered at zero frequency. The magnetic field pulse was applied along the detection axis using a Helmholtz coil, with a duration of 50 μs and amplitude of 117 μT, corresponding to the condition

$$|\gamma^1\mathrm{H} - \gamma^{15}\mathrm{N}|B_P t = \pi/2,$$

where B_P is the pulse field amplitude. A detailed description of the ZULF NMR experimental apparatus is given in Ref. [34].

This manuscript is based on the work done prior to February 2022.

Acknowledgments. I.V.K. thanks the Russian Science Foundation for financial support of the SABRE experiments (RSF grant 22-43-04426).

REFERENCES

1. B. Blümich, TrAC Trends in Anal. Chem. **83**, 2 (2016).

2. J. Mitchell, L. F. Gladden, T. C. Chandrasekera et al., Prog. Nucl. Magn. Reson. Spectrosc. **76**, 1 (2014).

3. *NMR Logging Applications,* in *Handbook of Geophysical Exploration: Seismic Exploratio*n, Vol. 32, ed. by K.-J. Dunn, D. J. Bergman, and G. A. Latorraca, *Nuclear Magnetic Resonance Petrophysical and Logging Applications*, Pergamon (2002), pp. 129–164.

4. M. P. Augustine, D. M. TonThat, and J. Clarke, Solid State Nucl. Magn. Reson. **11**, 139 (1998).

5. J. Meinel, M. Kwon, R. Maier et al., Commun. Phys. **6**, 302 (2023).

6. I. M. Savukov and M. V. Romalis, Phys. Rev. Lett. **94**, 123001 (2005).

7. M. C. D. Tayler and S. Bodenstedt, J. Magn. Reson. **362**, 107665 (2024).

8. D. B. Burueva, J. Eills, J. W. Blanchard et al., Angew. Chem. Int. Ed. **59**, 17026 (2020).

9. J. Eills, D. Budker, S. Cavagnero et al., Chem. Rev. **123**, 1417 (2023).

10. R. Picazo-Frutos, Q. Stern, J. W. Blanchard et al., Anal. Chem. **95**, 720 (2023).

11. T. Theis, P. Ganssle, G. Kervern et al., Nature Phys. **7**, 571 (2011).

12. C. R. Bowers and D. P. Weitekamp, J. Am. Chem. Soc. **109**, 5541 (1987).

13. R. W. Adams, J. A. Aguilar, K. D. Atkinson et al., Science **323**, 1708 (2009).

14. D. A. Barskiy, S. Knecht, A. V. Yurkovskaya et al., Prog. Nucl. Magn. Reson. Spectrosc. **114-115**, 33 (2019).

15. P. J. Rayner, M. J. Burns, A. M. Olaru et al., Proc. Natl. Acad. Sci. **114**, E3188 (2017).

16. R. V. Shchepin, D. A. Barskiy, D. M. Mikhaylov et al., Bioconjug. Chem. **27**, 878 (2016).

17. H. Zeng, J. Xu, J. Gillen et al., J. Magn. Reson. **237**, 73 (2013).

18. E. J. Fear, A. J. Kennerley, P. J. Rayner et al., Magn. Reson. Med. **88**, 11 (2022).

19. R. V. Shchepin, J. R. Birchall, N. V. Chukanov et al., Chem. Eur. J. **25**, 8829 (2019).

20. O. G. Salnikov, N. V. Chukanov, A. Svyatova et al., Angew. Chem. Int. Ed. **60**, 2406 (2021).

21. H. De Maissin, P. R. Gro, O. Mohiuddin et al., Angew. Chem. Int. Ed. **62**, e202306654 (2023).

22. K. MacCulloch, A. Browning, D. O. Guarin Bedoya et al., J. Magn. Reson. Open **16-17**, 100129 (2023).

23. T. Theis, M. P. Ledbetter, G. Kervern et al., J. Am. Chem. Soc. **134**, 3987 (2012).

24. J. W. Blanchard, B. Ripka, B. A. Suslick et al., Magn. Reson. Chem. **59**, 1208 (2021).

25. P. Put, S. Alcicek, O. Bondar et al., Commun. Chem. **6**, 1 (2023).

26. E. T. Van Dyke, J. Eills, R. Picazo-Frutos et al., Sci. Adv. **8**, eabp9242 (2022).

27. J. Dunn and A. Blight, Curr. Med. Res. Opin. **27**, 1415 (2011).

28. S. A. Dingsdag and N. Hunter, J. Antimicrob. Chemother. **73**, 265 (2018).

29. D. A. Barskiy, R. V. Shchepin, A. M. Coffey et al., J. Am. Chem. Soc. **138**, 8080 (2016).

30. D. O. Guarin, S. M. Joshi, A. Samoilenko et al., Angew. Chem. Int. Ed. **62**, e202219181 (2023).

31. A. I. Trepakova, I. V. Skovpin, N. V. Chukanov et al., J. Phys. Chem. Lett. **13**, 10253 (2022).

32. J. Osborne, J. Orton, O. Alem et al., Proc. SPIE **10548**, 105481G (2018).

33. J. Dupont-Roc, S. Haroche, and C. Cohen-Tannoudji, Phys. Lett. A **28**, 638 (1969).

34. J. W. Blanchard, T. Wu, J. Eills et al., J. Magn. Reson. **314**, 106723 (2020).

35. Q. Stern and K. Sheberstov, Magn. Reson. **4**, 87 (2023).

36. N. V. Chukanov, O. G. Salnikov, I. A. Trofimov et al., ChemPhysChem **22**, 960 (2021).

37. D. A. Barskiy, K. V. Kovtunov, I. V. Koptyug et al., J. Am. Chem. Soc. **136**, 3322 (2014).